

ORIGINAL ARTICLE

Vision Therapy in Adults with Convergence Insufficiency: Clinical and Functional Magnetic Resonance Imaging Measures

Tara L. Alvarez*, Vincent R. Vicci†, Yelda Alkan‡, Eun H. Kim§, Suril Gohel‡, Anna M. Barrett||, Nancy Chiaravalloti*, and Bharat B. Biswal*

ABSTRACT

Purpose. This research quantified clinical measurements and functional neural changes associated with vision therapy in subjects with convergence insufficiency (CI).

Methods. Convergence and divergence 4° step responses were compared between 13 control adult subjects with normal binocular vision and four CI adult subjects. All CI subjects participated in 18 h of vision therapy. Clinical parameters quantified throughout the therapy included: nearpoint of convergence, recovery point of convergence, positive fusional vergence at near, near dissociated phoria, and eye movements that were quantified using peak velocity. Neural correlates of the CI subjects were quantified with functional magnetic resonance imaging scans comparing random vs. predictable vergence movements using a block design before and after vision therapy. Images were quantified by measuring the spatial extent of activation and the average correlation within five regions of interests (ROI). The ROIs were the dorsolateral prefrontal cortex, a portion of the frontal lobe, part of the parietal lobe, the cerebellum, and the brain stem. All measurements were repeated 4 months to 1 year post-therapy in three of the CI subjects.

Results. Convergence average peak velocities to step stimuli were significantly slower ($p = 0.016$) in CI subjects compared with controls; however, significant differences in average peak velocities were not observed for divergence step responses ($p = 0.30$). The investigation of CI subjects participating in vision therapy showed that the nearpoint of convergence, recovery point of convergence, and near dissociated phoria significantly decreased. Furthermore, the positive fusional vergence, average peak velocity from 4° convergence steps, and the amount of functional activity within the frontal areas, cerebellum, and brain stem significantly increased. Several clinical and cortical parameters were significantly correlated.

Conclusions. Convergence peak velocity was significantly slower in CI subjects compared with controls, which may result in asthenopic complaints reported by the CI subjects. Vision therapy was associated with and may have evoked clinical and cortical activity changes.

(Optom Vis Sci 2010;87:E985–E1002)

Key Words: convergence insufficiency, vision therapy, vergence, traumatic brain injury, prediction, frontal eye fields, supplementary eye field, dorsolateral prefrontal cortex, cerebellum, brain stem

Convergence insufficiency (CI) is a common binocular dysfunction with a reported prevalence of 4.2 to 7.7% in the general population.^{1–5} Studies report that patients with traumatic brain injury (TBI) have a greater incidence rate. CI is

evident in up to 48% of veterans exposed to blast injuries^{6–8} and in about 40% of the civilian population with TBI, predominantly from motor vehicle accidents and falls.^{9–11} Symptoms include blurred vision, diplopia, eye strain, loss of concentration, frequent loss of place having to reread, reading slowly, difficulty in remembering what was read, sleepiness, and headaches.^{12–16} These symptoms negatively impact an individual's quality of life and daily activities such as schoolwork¹⁷ and employment.¹⁰ It translates into a significant cost burden for CI and CI after TBI for individuals and society as a whole (more than \$600 million annually, conservatively estimating \$100 of lost work time per person affected).

*PhD, †OD, ‡MS, §BS, ||MD

Department of Biomedical Engineering, New Jersey Institute of Technology, Newark, New Jersey (TLA, YA, EHK, SG), Department of Vision Rehabilitation, Kessler Institute for Rehabilitation, West Orange, New Jersey (VRV), Private Practice, Westfield, New Jersey (VRV), Department of Radiology, University of Medicine and Dentistry of New Jersey, Newark, New Jersey (SG, BBB), and the Stroke Research Laboratory (AMB) and the Neuropsychology and Neuroscience Laboratory (NC), Kessler Foundation, West Orange, New Jersey.

In recent years, several randomized clinical trials have been published comparing the effectiveness of treatments for CI in children and adults.^{13,18–22} These studies have used both symptoms and clinical signs as outcome measurements. The results of these studies demonstrate that office-based vision therapy with home reinforcement is the most effective treatment for CI in children and adults. However, these studies did not evaluate objective outcome measurements nor did they provide any information about the underlying physiological changes that may correspond with the improvements in clinical signs and symptoms.

This study is designed to provide data about changes in the dynamics of the vergence system using objective eye movement recordings and to quantify and correlate neural measurements with these objective outcome measures using functional imaging. This study is the first step toward understanding how vision therapy/orthoptics/vision rehabilitation adapts the underlying neurophysiology to have a sustained effect of reducing patients' asthenopic complaints from CI.

This investigation will test two hypotheses. First, we hypothesize that subjects with CI will have reduced convergence peak velocity compared with controls with normal binocular vision. CI patients commonly report fatigue, and one study has shown that fatigue decreases peak velocity.²³ We speculate that the reduced speed is related to the asthenopic complaints. Furthermore, several studies report a decrease in symptoms after vision therapy.^{13,16,24} Our second hypothesis is that convergence peak velocity will significantly increase after vision therapy and those changes will be related to modifications in the blood oxygenation level dependent (BOLD) signal from functional magnetic resonance imaging (fMRI). This would suggest that vision therapy may facilitate cortical adaptation and increased activity in the neural networks shown by other studies to be specialized for near space computations.^{25,26} Once the mechanisms of adaptation facilitated by vision therapy are understood, then current therapies can be improved for those who are not responsive to current therapies. For example, about 25% of patients were not classified as improved after office therapy with home reinforcement, assessed by symptoms and clinical measurements.¹² Hence, understanding adaptation of the vergence system can lead to the design of new therapies or modification of existing procedures for those patients who do not respond well to the therapies that have currently been validated.

MATERIALS AND METHODS

Subjects

Four female subjects (aged 20 to 26 years, mean age, 23 ± 1.7 years) with a diagnosis of CI participated in this study. Two subjects, S1 and S2, had no history of brain trauma and had never lost consciousness. Hence, we suspect they developed CI during the maturation of their visual system. Two subjects, S3 and S4, had a history of mild TBI. Subject S3 was hit by a truck at the age of 4 years and was unconscious for several hours. Subject S4 struck the back of her head when playing sports at the age of 8 years and lost consciousness for about an hour. The anatomical MRI scans did not show any lesions within any of the subjects' scans assessed by a neuroradiologist. Subjects S1, S2, and S4 were emmetropes, and subject S3 was a -1 diopter (D) myope whose refraction was

corrected throughout all testing. None had a history of psychological dysfunctions or disorders. All CI subjects were right handed, which is commonly noted to determine hemispheric dominance for functional imaging studies.

Thirteen controls with normal binocular vision participated for comparison (4 females, 9 males; 21 to 35 years, mean age, 25 ± 4 years). For the control subjects, 10 were emmetropes. The refractive correction of three controls was between -1.5 and -2.0 D. These subjects wore their corrective refraction throughout testing. For the control cohort with normal binocular vision, the nearpoint of convergence (NPC) break point was <6 cm with normal positive fusional vergence (PFV) at near.

Stereopsis was better than 70 sec arc for all subjects assessed by Randot stereopsis. None of the subjects participated in any form of vision therapy before this study, had any history of ocular disease, or was taking medication at the time of testing. Subjects with supranuclear forms of strabismus (the most common disturbance of the vergence system) were also excluded. All subjects gave informed consent after a verbal and written explanation of the experiment, which was approved by the University of Medicine and Dentistry of New Jersey and the New Jersey Institute of Technology Institution Review Boards in accordance with the Declaration of Helsinki.

Clinical Measurements

Static Measurements and Symptoms

There were five static clinical measurements quantified during this study. For the study of the four CI subjects participating in vision therapy, all static parameters were measured at four different times: before, midway, and after vision therapy as well as during a follow-up session 4 months to 1 year post-therapy. During this study, the examiners were unmasked, which may be a source of bias. Symptoms were also quantified.

Stereopsis. Stereopsis was assessed with the Bernell Stereo Randot test using the Randot circles (Bernell, South Bend, IN). The test consisted of eight grades that ranged from 20 to 400 sec arc. Normal was defined as better than 70 sec arc. All subjects had to discern 70 sec to be included in this study.

NPC Break Value. NPC was measured by having the operator slowly bring the tip of a pen toward the subjects along their midline. The subjects were instructed to concentrate on the pen tip and to keep it clear and single. When the pen tip doubled, the operator would stop and ask the subjects if they could make the object single. If the subject was able to fuse the target, then the operator would slowly move the pen closer. When the subject could no longer maintain fusion, the distance was measured. The distance from the subject's orbit to the pen tip was recorded in centimeter using a ruler as the NPC. The NPC was measured twice and averaged.

Recovery Point of Convergence. After the NPC was measured, the recovery point of convergence (RPC) was assessed. Once the tip of the pen was perceived as diplopic, the operator slowly withdrew the pen away from the subject along the midline. The subjects were told to try to fuse the pen tip and report when they were able to regain fusion. This distance was measured from the target position to the subject's orbit in centimeter using a ruler.

Near Fusional Vergence (Amplitudes at Near). Fusional vergence was measured using both base-out (BO) and base-in (BI) prisms with the Bernell horizontal prism bar (Bernell) to assess PFV and negative near fusional vergence, respectively. It contained 15 prisms: 1 Δ , 2 Δ through 20 Δ in increments of 2 Δ , and 20 Δ through 45 Δ in increments of 5 Δ . The subject held a pen that was placed 40 cm (measured with a ruler) away from midline. The subject was instructed to look at the pen tip and try to keep it clear and single. The operator held the prism bar over the right eye. A new prism was introduced about every 2 s, and the subject was asked to report when the pen tip first blurred and doubled. For some subjects, the target became diplopic, and the subject did not perceive blur. If the target doubled, the operator held the prism and asked the subjects if they could make the pen tip fused into one. When the subject could no longer maintain fusion, that prism was denoted as the break point. The prism strength was increased, and the subject was asked if the pen tip was still two. Then, the prism was decreased in strength waiting about 2 s per prism until the subject could view the pen tip as a single object. Results discussed below are reported for when the tip of the pen became diplopic or the break point.

Dissociated Near Phoria. The dissociated near phoria was assessed subjectively using a Maddox Rod with the Bernell Muscle Imbalance Measure (MIM) card (Bernell). This card has a resolution of 1 Δ and a range of 28 Δ exophoria to 28 Δ esophoria. The MIM card is calibrated for the right eye; hence, the phoria was measured with the left eye fixating on penlight shown through the card. The MIM card was placed at a measured 40 cm or 16 in away from the subject's midline, which equates to an accommodative demand of 2.5 D.

Symptoms. Symptoms were quantified using the Convergence Insufficiency Symptom Survey (CISS).¹³ The CISS is a 15-question survey. Each question or symptom is scored between 0 and 4 where 0 represents the symptom never occurs and 4 represents the symptom always occurs. The responses are summed where a score of 21 or higher has been validated to have a sensitivity of 98% and specificity of 87% in adults.²⁷ It has also been validated in children where investigators recommend a score of 16 or greater to differentiate children with symptomatic CI compared with controls.^{28,29} The symptoms of S4 were collected during testing. The symptoms of S1 through S3 were collected retrospectively, which is not ideal but because our subjects were adults, we felt they could remember their symptoms before vision therapy.

Dynamic Eye Movement Measurements Using Limbus Tracking System

Eye movements were recorded using an infrared ($\lambda = 950$ nm) limbus tracking system manufactured by Skalar Iris (model 6500; Delft, The Netherlands). All the eye movements were within the linear range of the system ($\pm 25^\circ$). The system has a high degree of linearity, within 3% between $\pm 25^\circ$ horizontally.³⁰ Digitization of the individual left eye and right eye movements were performed with a 12-bit digital acquisition hardware card using a range of ± 5 volts (6024 E series; National Instruments, Austin, TX) at a sampling rate of 200 Hz. Convergence and divergence 4° symmetrical step eye movement responses were recorded and compared between CI subjects and controls with normal binocular vision. For

the initial comparison, the baseline data from CI subjects were compared with one session from controls responding to 4° convergence and divergence symmetrical step stimuli. For the study of CI subjects participating in vision therapy, the eye movements stimulated during the office session are discussed below.

A custom Matlab version 2008 (Waltham, MA) program was used for all data analysis. Left eye and right eye movement data were converted into degrees using the individual calibration data. Calibration for vergence step responses was composed of two points, which were the initial and final position of the step or ramp stimuli. Vergence was calculated by subtracting the right eye movement from the left eye movement to yield a net vergence response. Blinks were easily identified based on manual inspection of the left and right eye movement responses. Responses with blinks at any point during the movement were omitted. Convergence responses were plotted as positive, whereas divergence responses were plotted as negative.

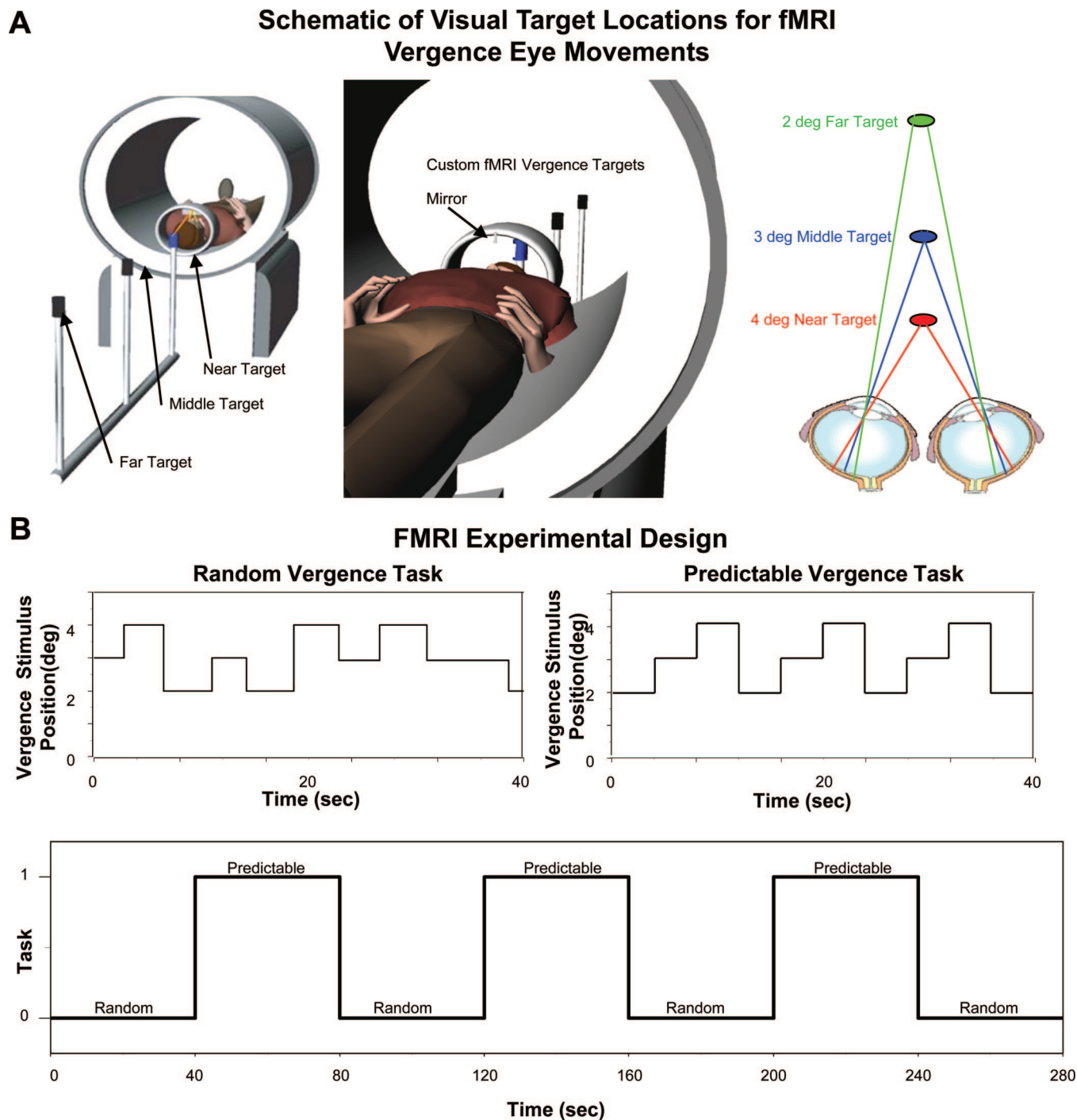
Vergence peak velocity was assessed using a two-point central difference algorithm to compute the vergence velocity response.³¹ The two-point central difference algorithm inherently filters the data. To ensure that the range used within the algorithm did not influence the peak velocity, only five data points were used in each velocity point calculation. The range of data points in the algorithm was adjusted between three and seven data points to determine if the range influenced the peak velocity. The peak velocity did not change using this range. Hence, a range of five data points does not introduce artifacts to the peak velocity calculation. Data were not further filtered. The maximum value of the velocity trajectory was the peak velocity.

Neural Correlate Measurements Using the BOLD Signal from Functional Imaging

Imaging Instrumentation

Images were acquired using a 3.0 Tesla Siemens Allegra MRI scanner with a standard head coil (Erlangen, Germany). All functional experiments were performed in the morning between 9:00 and 11:00 AM, and subjects were asked to keep to their normal routine for sleeping and eating to decrease variability between scans. Visual stimuli observed during the functional scanning were created by three custom light-emitting diodes (LEDs; dimension: 5 cm \times 2 mm; wavelength: 400 nm) secured with Polyvinyl Chloride (PVC) piping. The subjects were positioned supine on the gantry of the scanner with their head along the midline of the coil. All participants were instructed to limit head motion. A schematic of the visual stimuli with the subject is shown in Fig. 1 plot A. Foam padding was used to restrict additional movement, and motion correction software described below was used to ensure that head motion did not influence the results. Ear plugs that still enabled the participant to hear instructions from the operators were used to ensure communication during the scan while reducing scanner noise by up to 30 dB. In all experiments, the radio frequency power deposition and field-switching rate were kept below levels specified by the U.S. FDA.

A quick scan was obtained and used to localize high-resolution anatomical and functional scans within the magnet. Because the cerebellum and brain stem were areas of interest in this study, all subjects were positioned so that images of the whole brain could be

**FIGURE 1.**

(A) Schematic of custom fMRI compatible LED visual stimulator, which was symmetrically aligned along the subject's midline. The subject viewed the target using a mirror. (B) Experimental design showing the pattern of illumination for the three visual targets for the 40 s duration for a given page during the random phase followed by 40 s of a predictable vergence task using a standard block design. Vergence stimulus position is the combined stimulation to both eyes where vergence is denoted as the difference between the left eye and the right eye stimulus. Convergence is plotted as positive, and divergence is plotted as negative. A color version of this figure is available online at www.optvissci.com.

attained. All functional scans used a T2*-weighted echo planar imaging sequence. The imaging parameters were field of view = 220 mm, 64×64 matrix, repetition time = 2000 ms, echo time = 27 ms, and flip angle = 90° . The whole brain was imaged in an axial configuration where 32 slices were collected, and each slice was 5 mm thick. The resolution was $3.4 \times 3.4 \times 5$ mm. There were 140 volumes acquired per scan equating to a duration of 4

min and 40 s. Between scans, the subjects were asked if they were comfortable and could perform the task. Subjects confirmed that they could perform each task. After all functional tasks, a high-resolution magnetization-prepared rapid gradient-echo data set was collected. The magnetization-prepared rapid gradient-echo imaging parameters were 80 slices, field of view = 220 mm, slice thickness = 2 mm, repetition time = 2000 ms, echo time = 4.38

ms, $T1 = 900$ ms, flip angle = 8° , and matrix = 256×256 , which resulted in a spatial resolution of $0.9 \times 0.9 \times 2$ mm.

Functional Imaging Experimental Design

One commonality in therapy is repetition of movement where the magnitude, direction, and timing of the movement are known. When the magnitude, direction, and timing of a stimulus are known, prediction is stimulated. Prediction influences vergence movements by reducing the latency (movement onset) and increases the peak velocity in control subjects with normal binocular vision.^{32,33} We hypothesize that vision therapy will stimulate neural activity changes that can be detected using a prediction experimental protocol discussed below.

Functional scans were obtained with a standard block design using either a predictable or random vergence eye movement stimulus. During the random phase, one of the three LEDs, symmetrically located along the subject's midline, was illuminated for a random duration of time between 2 and 5 s. The vergence binocular demand was either 4° (near target), 3° (middle target), or 2° (far target), as shown in Fig. 1 plot A. About 10 vergence step stimuli were presented within each random phase. The subject could not anticipate the timing of the visual stimulus. For the prediction phase, illumination of the LEDs located at near (4°), at middle (3°), and at far (2°) was alternated sequentially so that the subject could anticipate the next visual stimulus. Each LED was individually illuminated for 4 s. Subjects could easily predict the direction, magnitude, and timing of the visual stimulus.

Random and predictable phases were repeated for 3.5 cycles for a total duration of 280 s or 4 min and 40 s. The subjects were instructed to look at the visual target and blink when needed without moving their heads. Subjects were instructed to anticipate the next target when they were in the predictable phase. Each subject was verbally told when to predict. A schematic of the visual stimulus is shown in Fig. 1 plot B.

Functional Image Analysis

Data were analyzed with AFNI.³⁴ All the scans were first registered and motion corrected. As with any fMRI data set, the data collected were susceptible to motion artifact from head motion or other non-neuronal influences.³⁵ Hence, all data used in this study were analyzed for the presence of motion-induced artifact. Subjects were instructed to limit head motion, and foam padding was used to further reduce motion. Many algorithms exist for the detection and correction of mis-registered images. For this study, a minimum least square image registration method available in AFNI was used to detect and correct for the presence of any motion-induced changes on the 3D image space. There were six parameters monitored to determine if head motion was a problem within our data set. Three parameters calculated the millimeter of movement within each plane (anterior to posterior, right to left, and inferior to superior), and three parameters calculated the amount of rotation in degrees between planes (yaw, pitch, and roll). AFNI's default is to calculate millimeter of movement within a plane and to calculate the degree of rotation between planes. Data were sync interpolated in time to account for phase shifts related to slice-wise data acquisition. Motion correction involved both the removal of spa-

tially coherent signal changes using a partial correlation method and the application of a six-parameter, rigid-body, least squares alignment routine. A recent comparison of several software packages found that the AFNI image registration algorithm was both reliable and fast in comparison with other software.³⁶ The least square image registration method used in this study used the fourth image in each data set as a reference, and the motion parameters were estimated for the time-series set. Head motion was not problematic in our data sets.

After motion correction, the data were detrended to eliminate linear drifts in the data set. Three trials were recorded in case head motion was problematic in our data set. Because head motion was minimal, the three vergence data trials were concatenated using all the three trials where each trial lasted for 4 min 40 s. Hence, the concatenated data set was 14 min in total. The fMRI BOLD signal analyzed using a general linear model (GLM) method has been reported to be correlated to direct neuronal measurements.^{37,38} Hence, the fMRI time series data within this study were analyzed with a GLM where each voxel of the entire brain was correlated with a hemodynamic model of our data set. Because of the variations of the hemodynamic response function, a data-driven independent component analysis was used to obtain a reference vector corresponding to the experimental stimulus.^{39–41} Probabilistic independent component analysis available through the MELODIC software from FSL was used to calculate the independent signal sources.⁴² The signal source that corresponded to our block design was the reference vector used to correlate each voxel within our data set. By using the GLM analysis, only data that attained a minimum threshold of functional activity corresponding to a z score of 2.6 and p value of 0.005 were further analyzed.

Individual anatomical and functional brain maps were transformed into the standardized Talairach-Tournoux coordinate space.⁴³ Functional data (multiple regression coefficients) were spatially low-pass filtered using a Gaussian kernel (6 mm full width half maximum) and then merged by combining coefficient values for each interpolated voxel across all participants. The combination of individual voxel probability threshold ($z = 2.6$, $p < 0.005$) and the cluster size threshold (11 voxels rounded to a volume of 650 mm^3 for our data set) yielded the equivalent of a whole-brain corrected for multiple comparison significance level of $\alpha < 0.001$. The cluster size was determined using the AFNI AlphaSim program.⁴⁴ This program estimates the overall significance level by determining the probability of false detection through Monte Carlo simulation. Through individual voxel probability thresholding and minimum cluster size thresholding, the probability of false detection is determined from the frequency count of cluster sizes. The program does assume that the underlying population of voxel intensity has a normal distribution. Our simulation used 10,000 Monte Carlo iterations, assumed a cluster connection of the nearest neighbor, voxel dimension of $3.4 \times 3.4 \times 5$ mm, and sought a threshold significance of $\alpha < 0.001$. Hence, a cluster size rounded to 650 mm^3 or greater corresponded to $p < 0.001$ corrected for multiple comparisons. Individual maps of t -statistics were smoothed with a Gaussian kernel of 6 mm full width, half maximum to account for interindividual anatomical variation.^{45–47} Only functional data that reached statistical significance ($p <$

0.001) were overlaid on top of the anatomical scan where the significance is denoted as a z score shown in the figure scale bar. The skull was removed because it is not relevant to our experiment.

Functional images were quantified using the functional spatial regions of interest (ROI) masks.⁴⁸ Five ROIs were chosen because they contained the following regions: (1) dorsolateral prefrontal cortex (DLPFC); (2) frontal lobe, specifically the frontal eye field (FEF), supplemental eye field (SEF), and medial frontal gyrus (MFG); (3) the parietal lobe that contained the precuneus, inferior parietal area, parietal eye field (PEF), and Brodmann areas 39 and 40; (4) the cerebellum; and (5) the brain stem. There were two main parameters used to quantify functional images: (1) spatial extent of significant activation and (2) the average correlation within a given ROI. Spatial extent was quantified by adding up the number of significantly active voxels within an ROI. The total number of active voxels was divided by the total number of voxels within an ROI to yield a percent of activity for a given ROI. The average correlation is the average correlation coefficient for a given ROI. Results for both spatial extent of activation within an ROI and the average correlation of a particular ROI were compared within each subject for the functional scan before and after vision therapy, as well as during a follow-up session between 4 months and 1 year post-training.

Training Protocol

Home-Based Training

The first two sessions of home training were supervised in the office to ensure that the subject was properly performing each task. There was a total of 18 h of therapy, 6 h at home and 12 h in the office. Home training entailed two 10-min sessions (morning and evening) 3 days per week for 6 weeks. Office training was 1 h sessions, twice per week for 6 weeks.

During the 18 d of home training, subjects used a Brock string and loose stick prism. The subject practiced accommodative convergence by using two Brock strings to perform two tasks. For the first task, the subject looked at three different beads located at fixed positions along midline to stimulate step responses. From the tip of the subject's nose, the first, second, and third bead were located 10, 30, and 45 in away, respectively. For the second task, the subject used a separate string with one end secured to an object and the other against the subject's nose held along midline. The subject moved and visually tracked a bead along midline inward and outward to stimulate ramp responses. The range of bead movement was from the tip of the nose to the subject's arm length. For the loose stick prism training, S2 used a 10 Δ prism, and S1, S3, and S4 used an 8 Δ prism. The prism strength was chosen based on if the subject could fuse text from a book with the prism. Each subject used the stick prism or Brock string for 10 min and alternated between morning and evening. When using the loose stick prism, the subject would read text from a book. The prism would be placed over one eye to stimulate different amounts of vergence demands analogous to a step stimulus. The subject would read a book while using a prism over one eye. The subject alternated the prism between three conditions: (1) BO and BI; (2) BO and plano (no prism); and (3) BI and plano for 1.5 min for each eye while reading text. A record log was kept by each subject to record any

difficulties encountered during the home training and help facilitate that home training was performed.

Office-Based Training

The office-based training consisted of step and ramp stimuli analogous to jump vergence and smooth vergence.⁴⁹ The step stimuli were convergent 2, 4, and 6° steps as well as 4° divergence steps shown along the subject's midline. The ramp stimuli were presented at 1 and 2°/s starting from 2° ending at 8° where convergence and divergence movements were stimulated, respectively. Green LEDs, 2 mm wide by 25 mm in height with a wavelength of 555 nm, were used as target stimuli (model MU07 part 5101; Stanley, London, OH). For steps, subjects saw stimuli starting at an initial position of 2 or 4° vergence demand along the subject's midline and were asked to track the illuminated target that stimulated an inward convergent movement of 2, 4, or 6°. The vergence range used was 2 to 8°. This range was chosen because some subjects reported diplopia for targets closer than an 8° fixation. A 4° divergence stimulus was also given from an initial 6° vergence position. All step stimuli were presented after a random delay of 0.5 to 2.0 s to avoid prediction.³² Data were acquired for 4 s to ensure adequate time was given to allow the subject to fuse the new target. Subjects performed approximately 25 min of step training per session.

Ramp stimuli were 1 and 2°/s from 2 to 8° fixation (converging stimulus) and then from 8 to 2° (diverging stimulus) fixation. Hence, for the 1°/s ramp, the visual stimulus was presented for 12 s, and for the 2°/s ramp, the visual stimulus was presented for 6 s. The ramp stimuli were presented using a haploscope. Two computer screens were used to generate a symmetrical disparity vergence stimulus along the subject's midline. The stimulus was a green vertical line, 2 cm in height and 2 mm in width with a black background. Two partly reflecting mirrors projected the two vertical lines from the computer screens into the subject's line of sight. Before the experiment, the stimuli from the computer screens were adjusted with the mirrors to calibrate the visual stimulus with real targets located at measured distances from the subject's midline. During the experiment, only the visual stimulus displayed on the computer screen was seen by the subject. The subject's head was restrained using a custom chin rest to eliminate head movement, thus avoiding any vestibular influences in the experiment. The subject performed approximately 25 min of ramp training per session.

Summary of Vision Therapy Protocol

To summarize, 12 h of office testing were conducted, about 1 h per session, twice per week. A combined total of 6 h of home training were performed, 10 min in the morning and 10 min in the evening, 3 days per week for 6 weeks. Subjects did not complete office and home training on the same day.

Statistical Analyses for Clinical Measurements and Neural Correlates from Functional Imaging Measurements

Comparison between Control and CI Subjects

A Student's t-test was used to compare the average peak velocity of the 4° symmetrical convergence and divergence step responses

from the four subjects with CI and the 13 control subjects with normal binocular vision.

Study of CI Subjects Through Vision Therapy. Four subjects participated in all the before and after sessions, and subjects S2 through S4 participated in a follow-up scan 4 months to 1 year post-therapy. For the static clinical parameter (NPC, RPC, PFV and negative fusional vergence at near, and near dissociated phoria), a repeated-measures analysis of variance (ANOVA) was used to study the interaction of the differences between the clinical parameters measured: (1) before, (2) midway, (3) after, and (4) 4 to 12 months postvision therapy. For the dynamic eye movement parameters, a paired t-test was used to compare the before vs. the after parameters for the average peak velocity of the 2 and 4° convergence steps as well as 4° divergence step responses. A paired t-test was also used when comparing the spatial extent and average correlation within the five ROIs quantified from the prediction functional imaging experiment for the four CI subjects studied. A repeated measures of ANOVA was used to compare the before, after, and 4 to 12 months postvision therapy parameters for subjects S2 through S4. The software used for analysis was the NSC2004 (Kaysville, UT). A linear regression analysis was conducted between the clinical and the functional imaging measurements using Axum (Cambridge, MA).

RESULTS

Comparison of Eye Movements between Controls with Normal Binocular Vision vs. CI Subjects

Convergence Eye Movements

Fig. 2A plots an ensemble of convergence responses from 4° symmetrical step stimuli from two of the controls and two of the CI subjects. The controls are able to fuse the new target within 500 ms compared with the CI subjects who needed up to 2 s to acquire the new target. Hence, the convergence transient response is much slower for the CI subjects. The differences in convergence eye movement dynamics (the change from fusing a far to near target) are quantified by measuring the peak velocity. The results of the eye movements from the CI subjects after vision therapy will be discussed below.

Divergence Eye Movements

Divergence eye movements with similar initial positions were recorded from controls and those with CI. Ensemble plots from two control subjects and two CI subjects (Fig. 2B) qualitatively show that divergence responses look similar between the two groups. Peak velocity was measured from these responses to determine if the peak velocity of divergence was significantly different between controls and CI subjects.

The peak velocities from 4° convergence and divergence steps were quantified for the control and CI subjects. The average peak velocities \pm one standard deviation are plotted in Fig. 3. A significant difference is observed between the average peak velocity of 4° convergence symmetrical steps from controls and those with CI ($t = 2.7$, $p = 0.016$). CI subjects had significantly slower peak velocities, thus requiring a longer amount of time to acquire a new target located in depth compared with control subjects with normal binocular vision.

Divergence peak velocity was not significantly different between the two cohorts of subjects ($t = 1.2$, $p = 0.30$).

Longitudinal Study of CI Subjects through Vision Therapy

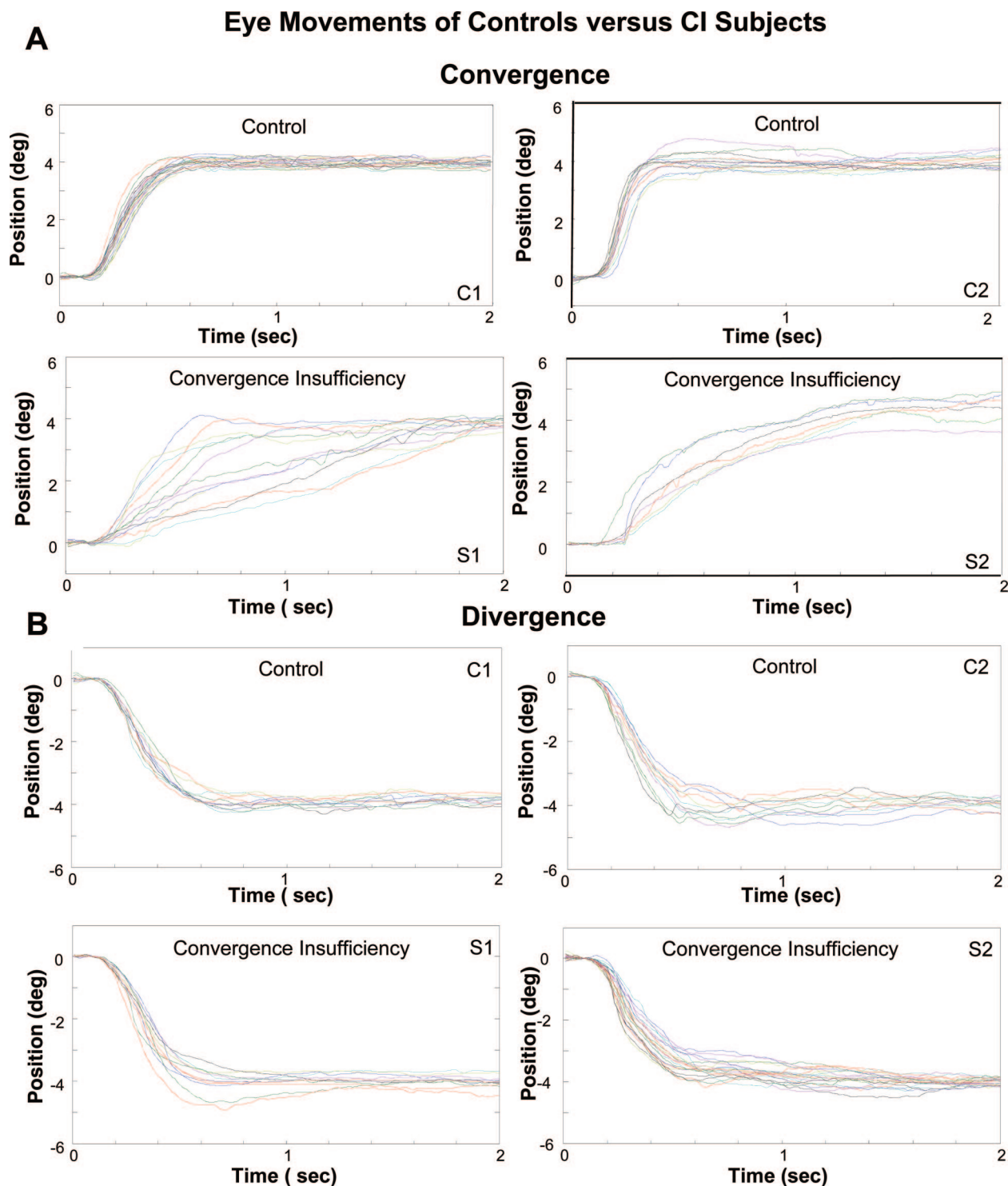
Static Clinical Measurements

Clinical parameters that significantly changed included: NPC, RPC, PFV at near, and near dissociated phoria. Measurements are plotted in Fig. 4 plots A, B, C, and D, respectively. The average and standard deviation for NPC, RPC, PFV and negative fusional vergence measured at near, near dissociated phoria, and CISS scores are tabulated in Table 1 before and after vision therapy, as well as the change between parameters.

When comparing NPC from the initial, midway, and final session using four subjects, there was a significant change in the (1) NPC [$F_{(2,6)} = 10.72$, $p < 0.01$]; (2) RPC [$F_{(2,6)} = 8.63$, $p = 0.02$]; (3) PFV at near [$F_{(2,6)} = 37.71$, $p < 0.001$]; and (4) near dissociated phoria [$F_{(2,6)} = 28.29$, $p < 0.001$]. Post hoc analysis using a Bonferroni all pairwise test indicated that the initial NPC, RPC, PFV at near, and near dissociated phoria were significantly different from those measured midway and after vision therapy for the four subjects studied. When comparing clinical parameters with four observations (initial, midway, after, and follow-up session) for subjects S2 through S4, a significant change was observed in (1) NPC [$F_{(3,6)} = 4.50$, $p = 0.05$]; (2) RPC [$F_{(3,6)} = 5.20$, $p = 0.04$]; (3) PFV at near [$F_{(3,6)} = 25.32$, $p < 0.001$]; and (4) near dissociated phoria [$F_{(3,6)} = 14.88$, $p = 0.003$]. Post hoc analysis using a Fisher LSD multiple-comparison all pairwise test specified that the initial baseline NPC, RPC, PFV at near, and near dissociated phoria were significantly different from the corresponding parameters measured midway and after vision therapy. This difference was also observed during the follow-up visit for the three subjects who participated in the follow-up session. NPC was closer toward the subject, and once the target became diplopic, the RPC also decreased after vision therapy. The PFV at near increased, and the dissociated near phoria became less exophoric after vision therapy. BI or negative fusional vergence at near decreased slightly, but the decrease was not significant within the four CI subjects studied. A Student's t-test of the CISS score showed a significant difference when comparing the before vs. after therapy survey ($p < 0.016$) where symptoms decreased after vision therapy.

Eye Movement Measurements

Fig. 5 plots the average vergence position traces from the first week of training (blue line), the last week of training (green line), and from the follow-up session (red line). For all four CI subjects, the average 2 and 4° convergence response (upper and middle rows, respectively) and average 4° divergence response (bottom row) were plotted. All four CI subjects participated in the 18 h of vision therapy. A follow-up session was recorded (red line) for S2 through S4. The transient portion of the position trace was faster after vision therapy for all four subjects. This change was quantitatively studied by measuring the response peak velocity. The 6° step responses had many blinks and large saccades that obstructed

**FIGURE 2.**

(A) Position responses ($^{\circ}$) as a function of time (sec) from 4° convergence symmetrical steps with similar initial positions from two control subjects with normal binocular vision and from two CI subjects. The CI subjects have slower transient movements compared with the controls. (B) Position responses ($^{\circ}$) as a function of time (s) from 4° divergence symmetrical steps with similar initial positions. The upper traces are from control subjects, and the lower traces are from CI subjects. Divergence eye movements are similar between the two cohorts of subjects. A color version of this figure is available online at www.optvissci.com.

the peak velocity of the movement. Hence, 6° responses were not quantitatively analyzed.

Fig. 6 quantifies the change in peak velocity dynamics in a bar plot showing the average \pm one standard deviation of the responses

collected from the first (white bar) and last (light gray bar) week of vision therapy for subjects S1 through S4 and during a follow-up session (dark gray bar) for subjects S2 through S4. For convergence responses, the average peak velocity increased after vision therapy

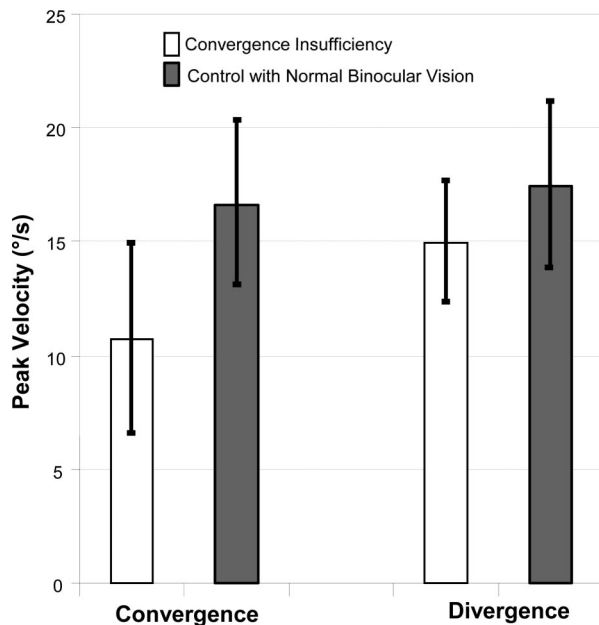


FIGURE 3.

Average peak velocities \pm one standard deviation from 4° convergence steps (left) and 4° divergence steps (right) from subjects with CI (white) and controls with normal binocular vision (gray). Convergence is significantly slower in the four CI subjects compared with the 13 controls. Conversely, no significant difference is observed with divergence.

whereas a consistent change was not observed for divergence movements. Using a paired t-test, a trend was observed for the 2° steps ($t = 2.6$, $p = 0.08$), and a significant difference was observed for the 4° steps ($t = 4.8$, $p = 0.017$). The divergence step average peak velocity did not change significantly ($t = 0.17$, $p = 0.9$). When analyzing peak velocity with an ANOVA between the three subjects (S2 through S4) who participated in the three sessions (first week, last week, and follow-up), a trend was observed but did not reach statistical significance for the 2° convergence responses [$F_{(2,4)} = 4.41$, $p = 0.1$] and 4° steps [$F_{(2,4)} = 3.67$, $p = 0.1$]. For the divergence steps, a significant difference was not observed [$F_{(2,4)} = 0.82$, $p = 0.5$].

Neural Correlate Measurements from Functional Imaging Using a Prediction Experiment

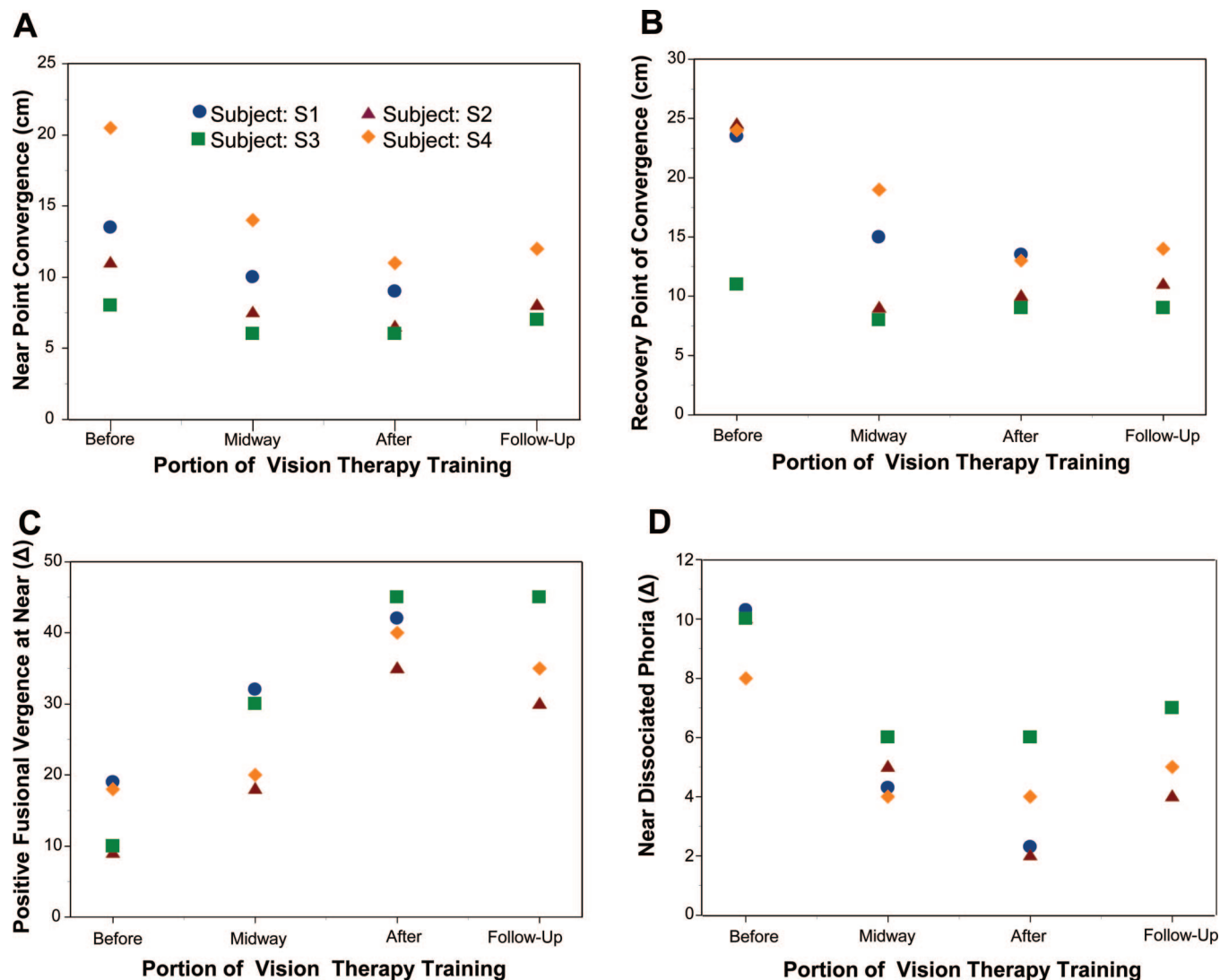
Differences were also observed within the fMRI images comparing the before and after vision therapy scans. An example of an axial and midsagittal image is shown for the four CI subjects where functional data are averaged across the data set. Each image is labeled to designate the before and after vision therapy, and the follow-up session (Fig. 7). For this study, a within-subject design was used, and the image analysis and visual stimulus were identical for all subjects during all scans. Experiments were also conducted at the same time of the day, and subjects were asked to keep their routine, especially the number of hours of sleep and diet, as consistent as possible. Hence, we attribute changes in the data set to be mostly from the vision therapy. Two trends were observed. First, the amount of significant activation increased during the after and follow-up sessions compared with the before vision therapy scan. Second, the cor-

relation, and hence z score significance, was greater as seen by more yellow color in the functional images. These data were then quantified to determine if consistent and significant trends were observed attributed to the vision therapy protocol.

Fig. 8 quantifies the fMRI images by measuring the percentage of significantly active voxels in a specified ROI (plot A) and calculating the average correlation and hence z score significance for a given ROI (plot B). Because each ROI had a different volume, we normalized the ROIs quantifying the percentage of significant activity for a given ROI. As with the eye movement measurements, there were two types of statistical analyses used. By using a paired t-test for the four CI subjects, there were significant changes in the DLPFC ($t = 4.86$, $p = 0.02$), the frontal lobe containing FEF, SEF, and MFG ($t = 3.27$, $p = 0.05$), the cerebellum ($t = 3.13$, $p = 0.05$), and the brain stem ($t = 3.51$, $p = 0.04$). The amount of significant activity or spatial extent significantly increased after vision therapy. A trend was observed within the parietal lobe containing the PEF, Brodmann areas 39/40, and the inferior parietal area ($t = 2.58$, $p = 0.08$).

An ANOVA was calculated to study the interactions among the initial scan, the scan after vision therapy, and the follow-up scan of the three subjects (S2 through S4) who participated. The following areas showed a significant increase in the amount of activity or spatial extent: (1) DLPFC [$F_{(2,4)} = 37.53$, $p = 0.003$]; (2) the frontal lobe containing the FEF, supplementary eye field (SEF), and MFG [$F_{(2,4)} = 7.9$, $p = 0.04$]; (3) the cerebellum [$F_{(2,4)} = 7.42$, $p = 0.05$]; and (4) the brain stem [$F_{(2,4)} = 8.37$, $p = 0.04$]. The areas within the parietal lobe showed a trend in the differences in the percentage of activity but did not reach statistical significance [$F_{(2,4)} = 5.09$, $p = 0.08$]. The amount of activation increased after the vision therapy compared to the initial baseline scan. Post hoc analysis using a Fisher all pairwise test indicated that the activity of both the DLPFC and the cerebellum during the baseline measurement was significantly different from the activity measured after vision therapy and during the follow-up scan. However, differences were not observed between the two scans after therapy (i.e., the one immediately following therapy and the one measured between 4 months and 1 year post-therapy). Fisher multiple-comparison test showed significant differences between the before and after scan studying the ROI within the frontal lobe that contained the FEF, SEF, and MFG and the brain stem but not between the before and follow-up scan.

The second method to quantify the fMRI data was to compute the average correlation of a given ROI, shown in Fig. 8 plot B. Using a paired t-test comparing the initial baseline correlation within the ROI with the average correlation within an ROI after vision therapy for the four CI subjects studied, the following areas showed significant changes: (1) DLPFC ($t = 3.50$, $p = 0.01$); (2) the area within the frontal lobe containing FEF, SEF, and MFG ($t = 3.87$, $p = 0.03$); (3) the area within the parietal lobe containing PEF, the inferior parietal area, and Brodmann areas 39/40 ($t = 3.17$, $p = 0.05$); (4) the cerebellum ($t = 3.66$, $p = 0.04$); and (5) the brain stem ($t = 3.89$, $p = 0.03$). The average correlation within the ROI increased after vision therapy. The ANOVA analyzing the interaction between the data before and after vision therapy and during a follow-up scan for the three subjects studied also showed significant differences for the following areas: (1) DLPFC [$F_{(2,4)} = 32.6$, $p = 0.003$]; (2) the area within the frontal

**FIGURE 4.**

Clinical measurements included the NPC (plot A), RPC (plot B), PFV at near using a BO prism bar (plot C), and near dissociated phoria (plot D), which were measured before, midway, after therapy, and during a follow-up visit. All subjects were exophoric. S1 was unable to return for the follow-up visit. These measurements are the absolute values and not the change in parameters. The change in parameters is found in Table 1. A color version of this figure is available online at www.optvissci.com.

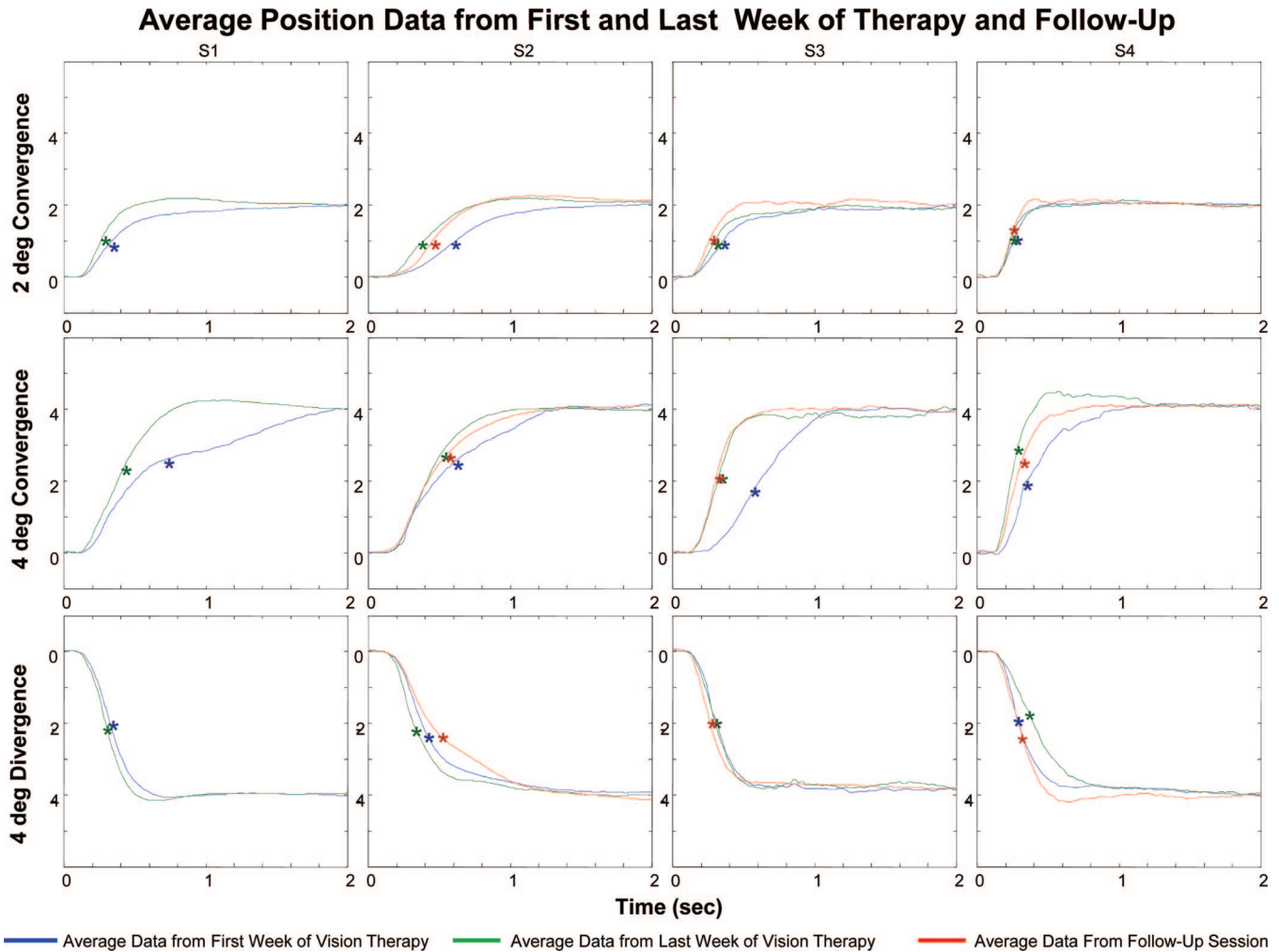
TABLE 1.

Average and standard deviation of clinical measurements before and after vision therapy with the change in parameters

| Variable | Before vision therapy | After vision therapy | Absolute value of change in parameter |
|---|-----------------------|----------------------|---------------------------------------|
| NPC (cm) | 13.4 ± 5.6 | 8.1 ± 2.3 | 5.3 ± 3.4 |
| RPC (cm) | 20.8 ± 6.5 | 11.4 ± 2.2 | 9.4 ± 5.3 |
| PFV at near using a BO prism bar (break) (Δ) | 14 ± 4.5 | 40 ± 4.1 | 26 ± 6.2 |
| Negative fusional vergence at near using a BI prism bar (break) (Δ) | 13.9 ± 1.7 | 12.0 ± 3.7 | 1.9 ± 2.6 |
| Near dissociated phoria (all subjects are exophores) (Δ) | 9.0 ± 1.4 | 3.3 ± 1.9 | 5.8 ± 2.1 |
| CISS | 26 ± 7 | 10 ± 5 | 16 ± 10 |

lobe containing FEF, SEF and MFG [$F_{(2,4)} = 9.05$, $p = 0.03$]; (3) the area within the parietal lobe containing the inferior parietal area, PEF, and Brodmann areas 39/40 [$F_{(2,4)} = 7.73$, $p = 0.04$]; (4) the cerebellum [$F_{(2,4)} = 7.39$, $p = 0.05$]; and (5) the brain stem

[$F_{(2,4)} = 11.50$, $p = 0.02$]. A post hoc Fisher LSD multiple comparison test shows a significant difference between the before and after scan as well as between the before and follow-up scan within (1) the DLPFC, (2) the frontal lobe ROI containing FEF, SEF,

**FIGURE 5.**

Plots of the average vergence position vs. time trace from the first week (blue), last week (green), and during a follow-up session (red). Convergence movements from 2° (top row) and 4° (middle row) step stimuli show that CI subjects can fixate on the new target faster after than before vision therapy. Average divergence 4° (bottom row) responses are shown for each session, and consistent changes are not observed. The asterisks denote the peak velocity for each trace.

and MFG, (3) the area within the parietal lobe containing the inferior parietal area, PEF, and Brodmann areas 39/40, (4) the cerebellum, and (5) the brain stem. The average correlation increased in the after and follow-up scans compared with the initial scan. Significant differences were not observed between the after vision therapy and follow-up scans.

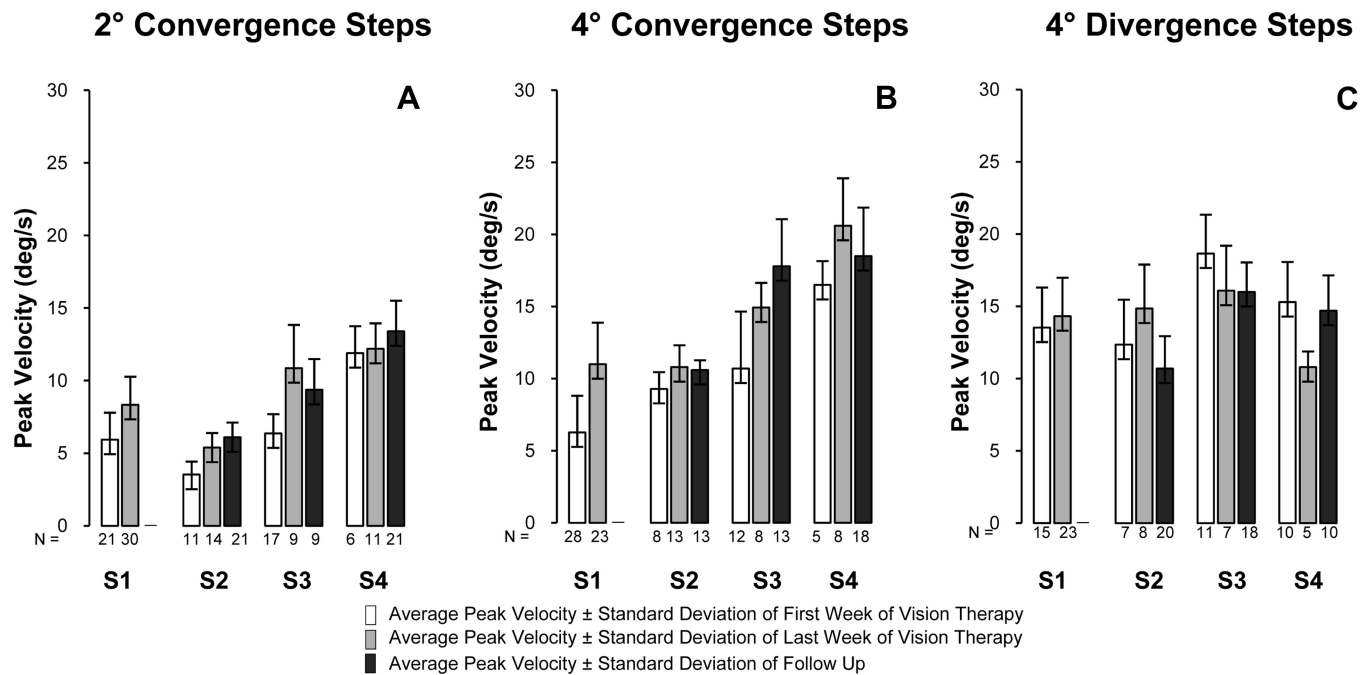
Summary of Statistical Differences

To summarize, numerous parameters showed significant differences ($p < 0.05$) when comparing the baseline measurements with those after 18 h of vision therapy. Both NPC and RPC decreased. The PFV at near increased, and the dissociated near phoria became less exophoric. The symptoms quantified via the CISS significantly decreased. The 4° convergent steps became significantly faster quantified via peak velocity. There was a significant increase in spatial extent and average correlation in the following ROIs: (1) DLPFC, (2) region containing FEF, SEF and MFG, (3) cerebellum, and (4) brain stem. The average correlation of the parietal area

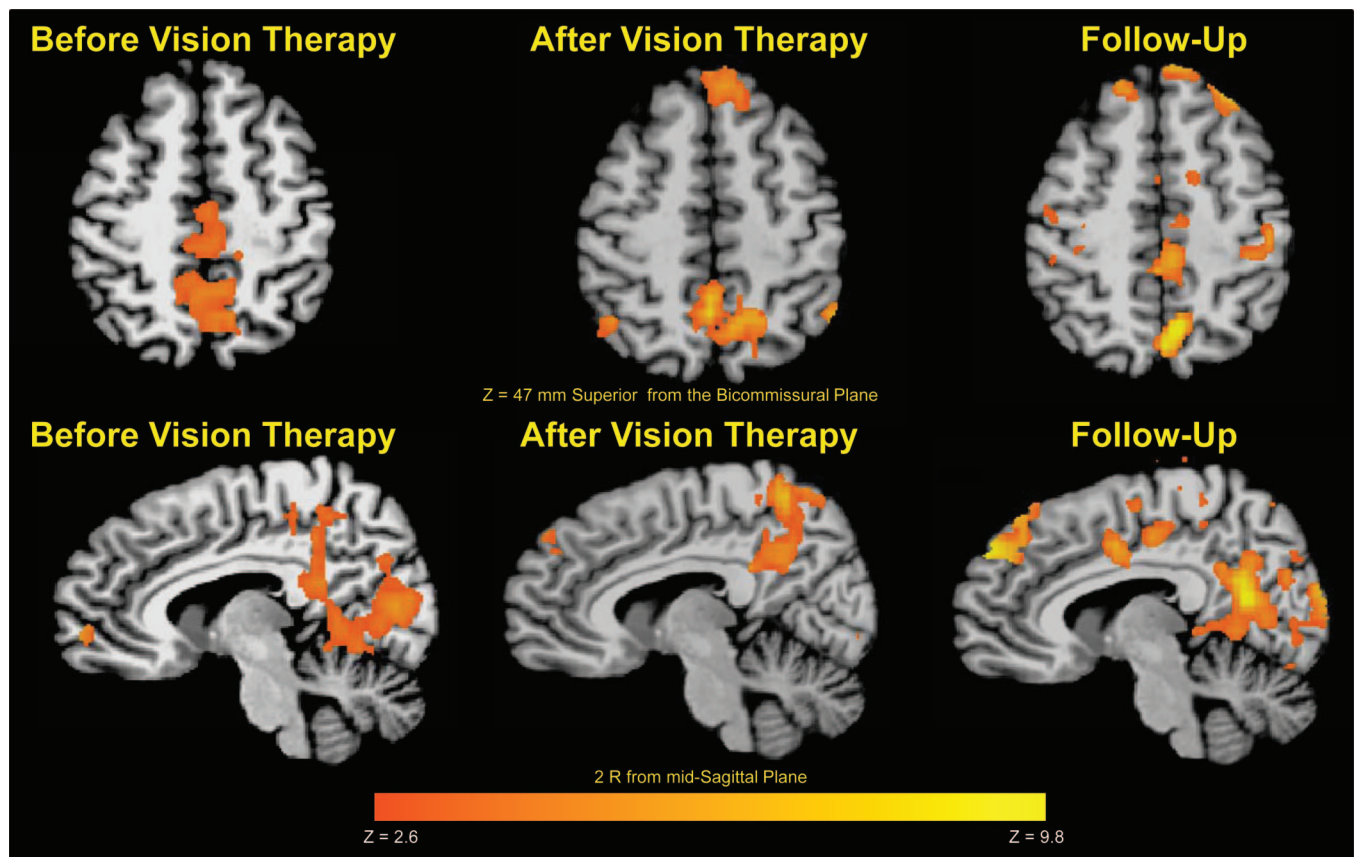
significantly increased in the ROI containing the PEF, precuneus, and Brodmann areas 39/40.

Linear Regression Studying Correlation between Clinical and Functional Imaging Parameters

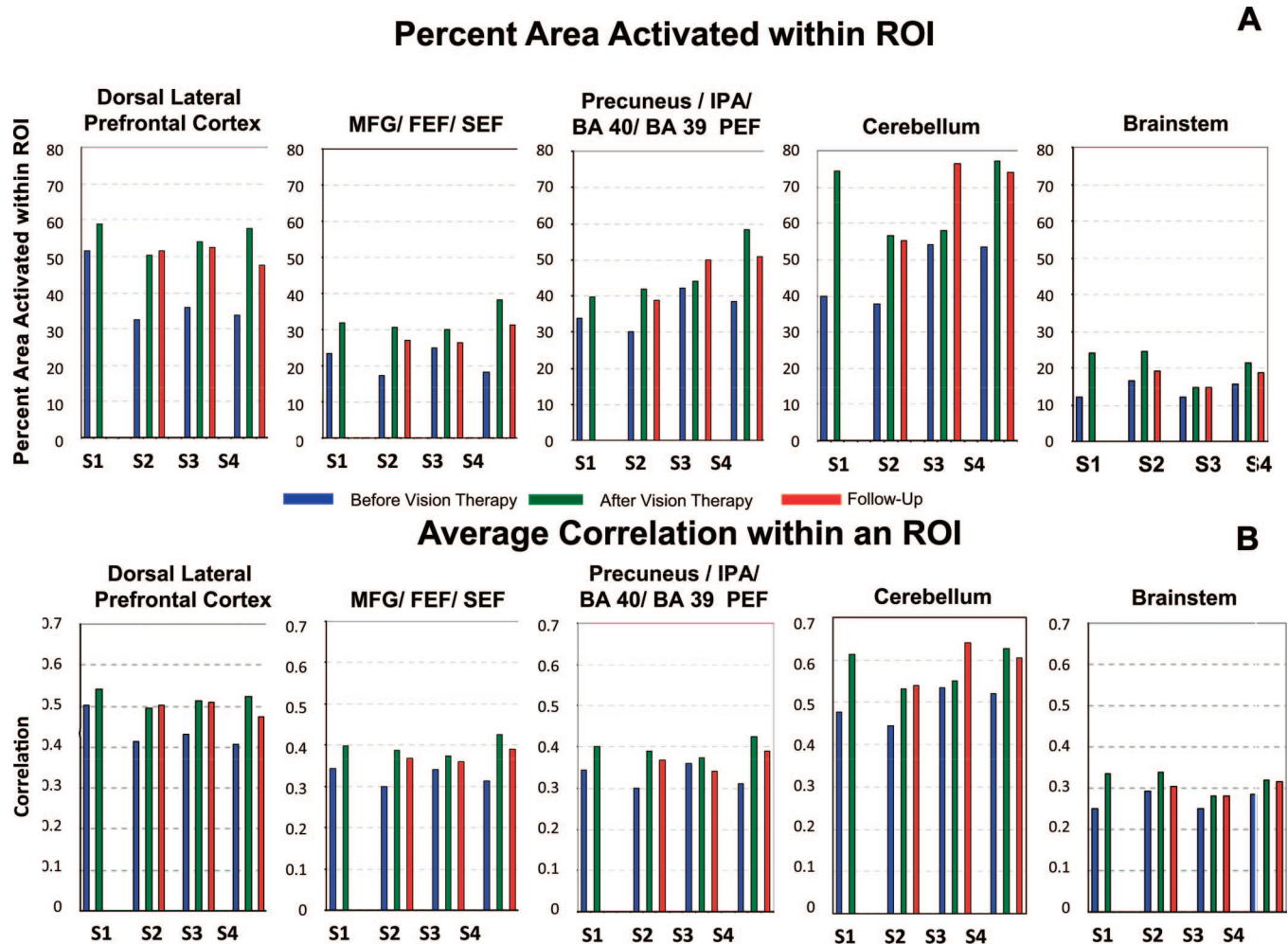
Linear regression analyses were performed between the clinical parameters and the functional imaging parameters as shown in Fig. 9. Parameters that were strongly correlated are plotted in red, and parameters that were weakly correlated are plotted in blue as denoted by the color bar. Several interesting findings were observed with the linear regression analyses. After vision therapy, all four subjects reduced their NPC (the subject could perceive an object as a single clear image closer to their midline), RPC, and near dissociated phoria. There was also more activity within the frontal lobe, brain stem, and cerebellum. The NPC was significantly correlated with the percentage of activity from the brain stem ($r = 0.64$, $p = 0.03$) and the average correlation of the brain stem ($r = 0.65$, $p = 0.03$) but not with any other region ($p > 0.1$). RPC was only

**FIGURE 6.**

Average peak velocity \pm one standard deviation for subjects S1 through S4 for 2° convergence (plot A), 4° convergence (plot B), and 4° divergence (plot C) responses from the first week of training (one bar), last week of training (light gray bar), and during a follow-up session (dark gray bar). The number of responses analyzed is denoted under each bar.

**FIGURE 7.**

Axial and sagittal view of data from functional imaging experiment studying prediction for four CI subjects. Images on the left column are the average of the before vision therapy data set, the middle column are after vision therapy, and the right column are from a follow-up scan. On average, increases in spatial extent (amount of significant activation) and/or intensity are observed when comparing the before and after scans.

**FIGURE 8.**

Longitudinal fMRI analysis of CI subjects S1 through S4. (A) Quantification of the percentage of voxels within an ROI showed that they were statistically significant during the fMRI experiment. Results show an increase in spatial extent when comparing data from before vision therapy (blue) with after vision therapy (green) and during the follow-up visit (red). For the five ROIs studied noted in the header of each plot, the spatial extent increased after training for all four CI subjects. (B) Average correlation of each ROI during the fMRI experiment showing an increase in correlation within an ROI from before vision therapy (blue) to after vision therapy (green) and during the follow-up visit (red). IPA, inferior parietal area; BA, Brodmann area.

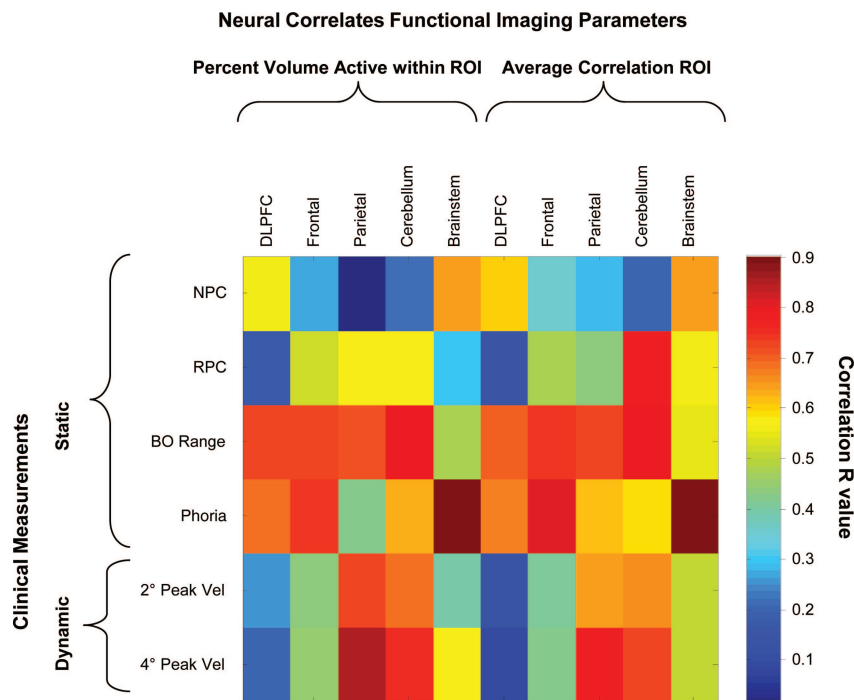
correlated with activity within the cerebellum ($r = 0.57$, $p = 0.06$ for percent activation within ROI and $r = 0.78$, $p = 0.05$ for average correlation within ROI). PFV at near was strongly correlated with the frontal, parietal, and cerebellar regions but not the brain stem. Near dissociated phoria was significantly correlated with the functional activity in the brain stem ($r = 0.90$, $p < 0.0001$ for percent activity within ROI and $r = 0.90$, $p < 0.0001$ for average correlation within ROI); the frontal ROI containing FEF and SEF ($r = 0.75$, $p = 0.008$ for percent activity within ROI and $r = 0.82$, $p = 0.002$ for average correlation within ROI), the DLPFC ($r = 0.69$, $p = 0.02$ for percent activity within ROI and $r = 0.67$, $p = 0.02$ for average correlation), and the cerebellum ($r = 0.63$, $p = 0.04$ for percent activity within ROI and $r = 0.59$, $p = 0.05$ for average correlation). Phoria was not correlated with the ROI in the parietal lobe.

More correlation was observed between the changes in the 4° vergence steps and functional imaging parameters throughout therapy compared with the 2° vergence steps. The average 4° step peak velocity was significantly correlated to the percentage of ac-

tivity within the ROI or spatial extent for the parietal area studied ($r = 0.86$, $p < 0.001$) and the cerebellum ($r = 0.76$, $p < 0.01$), as well as the average correlation within the parietal area studied ($r = 0.79$, $p < 0.01$) and the cerebellum ($r = 0.73$, $p = 0.01$). A trend was observed between vergence average 4° peak velocity and the brain stem percentage of activity ($r = 0.58$, $p = 0.1$) and the frontal ROI containing FEF and SEF percentage of activity ($r = 0.45$, $p = 0.16$). Significant trends were not observed between the DLPFC and the average 4° peak velocity ($p > 0.5$).

DISCUSSION

The results of this study provide the first published data demonstrating the effect of vision therapy on both objective eye movement and functional imaging outcome measurements. It further investigates the correlation between clinical and functional imaging parameters to gain insight as to how vision therapy is adapting the underlying neurophysiology.

**FIGURE 9.**

Linear regression analysis of clinical parameters vs. the functional imaging parameters (percent activation within an ROI and average correlation within an ROI). Clinical parameters include NPC, RPC, BO positive vergence range (BO range), near dissociated phoria, average 2° peak velocity (2° PeakVel), and average 4° peak velocity (4° PeakVel). Imaging parameters are the percent volume active within an ROI and average correlation for five ROIs studied. The correlation value is denoted in the scale bar. Parameters that are strongly correlated are plotted in red whereas parameters that are weakly correlated are plotted in blue.

Clinical Significance of Changes in Clinical Measurements

The Convergence Insufficiency Treatment Trial (CITT) classified patients as successful or improved using three outcome measurements.^{12,50} Successful was defined as a score < 16 on the CISS, a normal NPC (<6 cm), and normal PFV (>15 Δ). Improved was defined as a score < 16 on CISS or a 10-point decrease in CISS and at least one of the following: normal NPC, improvement of NPC more than 4 cm, normal PFV, or an increase in PFV of more than 10 Δ. For the four CI subjects studied within this investigation, S2 and S3 would be classified as successful and S4 would be improved. For S1, her CISS score was initially 24 before vision therapy and was 19 after therapy. Three of the four subjects would be classified as improved or successful based on CITT's definition. The Cohen d effect size of this data set for NPC and PFV was 1.2 and 6.4, respectively, which are considered large effect sizes. One study suggests that an effect size of 0.5 is a conservative estimate of a clinically meaningful difference.⁵¹ Hence, we believe the changes in clinical parameters observed within this study were clinically significant.

The sample of subjects within this study did show similar findings to the clinical trial published by CITT.¹² We observe a slightly greater increase in PFV at near and a smaller change in NPC compared with the CITT office-based vergence accommodation therapy (OBVAT) with home reinforcement results. The changes in the CISS scores for this study were comparable with their OBVAT pilot study and greater than the OBVAT clinical trial. We attribute the small differences in clinical measurements between the two studies to either one or a combination of the following: (1)

differences in the ages of the subjects between the studies, (2) differences in type of vision therapy administered (our study did not actively train accommodation), (3) differences in the accommodative target used to measure NPC and PFV at near, and (4) differences in the sample sizes of each study.

Near Dissociated Phoria vs. Functional Imaging

The near dissociated phoria is more controversial compared with NPC or PFV at near. Some investigators report no significant change⁵² whereas others report significant decreases.^{15,53} Our subjects showed significant decreases in near dissociated phoria, which was very significantly correlated to the functional activity of the brain stem and significantly correlated to the functional activity within DLPFC, cerebellum, and the frontal lobe region containing FEF and SEF but not correlated to the ROI within the parietal area. One study reports that lesions in the human cerebellum result in a decrease or loss of horizontal phoria adaptation.⁵⁴ In primates, evidence exists that phoria adaptation resides in the cerebellum vermis VI/VII or the "oculomotor vermis."⁵⁵ Cells referred to as the near response cells have been identified within the midbrain of primates that modulate their firing rate with phoria adaptation.⁵⁶ Hence, there is evidence in the literature suggesting cells in the cerebellum and/or the midbrain encode for phoria adaptation. The changes in the BOLD signal from the prediction experiment in this study could represent cortical changes that correlate to the decrease in near dissociated phoria. These changes in phoria may also impact vergence dynamics. For instance, our group has reported correlations between phoria and vergence dynamics.^{57–60}

Eye Movement Responses vs. Functional Imaging

Initially, CI subjects had slower peak velocity quantified from 2 and 4° convergent step stimuli compared with controls with normal binocular vision. One report states that the diagnosis of CI is challenging and suggests using eye movement dynamics as part of the diagnostic criteria because those with CI in their study had significantly reduced vergence movements compared with control subjects.⁶¹ Our CI subjects also had slower vergence dynamics compared with controls. We hypothesize that the decreases in vergence dynamics in patients who suffer from CI are potentially from reduced functional cortical activation. Furthermore, we speculate that a change in vergence dynamics after vision therapy may be due to more neurons becoming involved in the task (i.e., neuronal recruitment) and/or from those neurons firing their action potentials in more unison (i.e., neuronal synchronization).

Our results support that there is an increase in the amount of active voxels and the average correlation within the brain stem, cerebellum, and frontal lobe ROI containing FEF and SEF after vision therapy and these changes are correlated to an increase in vergence peak velocity. We speculate that the increase in functional activity represents a neuronal recruitment strategy and the increase in average correlation represents both recruitment of neurons and better synchronization of metabolic demand from the neurons. Because the functional imaging experiment was executed and analyzed using the same procedure, we attribute the changes observed within each subject to the 18 h of vision therapy. Although not fully overlapping with the dorsal visual functional regions identified with visual computations in near space in previous studies,^{25,26} nevertheless, cortical activity increases associated with therapy were located in regions likely to participate in a collicular-cortical dorsal visual network⁶² and may reflect increased processing of visual material specific to near space.

Primate and human case studies yield insight into the role of the cerebellum in vergence movements. For example, one study injected muscimol into the cerebellum vermis VI/VII of primates, which resulted in a decrease in convergence velocity and a “convergence insufficiency.”⁶³ Another report shows that the dorsal vermal outputs of the cerebellum are sent to the midbrain via the caudal fastigial nucleus.⁵⁵ Furthermore, human case studies report reduced vergence dynamics in those with cerebellar lesions, particularly those within the vermis.⁶⁴ Hence, evidence exists in both primate studies and human case reports that both the midbrain of the brain stem and the cerebellum, which are interconnected, are involved in vergence movements. Cells have also been identified within the frontal lobe, which modulate their activity with vergence stimuli. Single cell recordings from primates reveal a distinct area within the bilateral FEFs that is allocated for step vergence responses and is located more anterior compared with the cells responsible for saccadic signaling.⁶⁵ The fMRI studies also report differentiation of functional activity between saccadic and vergence eye movements within the FEF studying humans.⁶⁶ These regions (the brain stem, cerebellum, and frontal lobe) all showed changes within this study, which were correlated to the changes in peak velocity 4° convergence step responses.

Comparison between Subjects with CI and Controls with Normal Binocular Vision

This study shows that CI subjects have significantly slower convergence responses to 4° symmetrical step stimuli compared with controls. However, their divergence responses to 4° symmetrical step stimuli are not significantly different from controls. Another study comparing CI with control subjects showed that control subjects initiated significantly greater convergence gain (response amplitude/stimulus amplitude) when using a 7.7° symmetrical step stimulus compared with CI subjects.⁶¹

Different cells fire for convergence and divergence⁶⁷; therefore, there is no reason for the systems to be identical. Other results support differences between convergence and divergence responses. For step responses, the dynamics of divergence steps were dependent on the initial position of the stimulus, but convergence responses did not exhibit a significant initial position dependency.^{32,68} For ramp responses, as the stimulus moved further away from the subject along the cyclopean axis, the divergence velocity significantly decreased compared with responses closer to the subject.^{59,69,70} Clinical studies report that divergence, but not convergence velocity to ramp targets, was reduced in subjects with acute cerebellar lesions from ischemic strokes compared with controls suggesting separate cells control convergence and divergence movements within the cerebellum.⁶⁴ Our current findings support that the dynamics of convergence movements can be reduced while divergence movements remain normal in those with CI compared with controls providing more support that convergence and divergence are separate systems.

Study Limitations

Retrospectively, all subjects should have had their symptoms quantified using the CISS during the vision therapy. The CISS has been validated in adults²⁷ and children²⁸ and was developed through the randomized clinical trials of the CITT. CISS has also been used in another study of CI to evaluate therapeutic outcomes.⁷¹ Lack of a placebo therapy and a control cohort with normal binocular vision participating in vision therapy are also current limitations of this study. Only with a placebo or control vision therapy, can we accurately determine if functional changes are due to vision therapy changes vs. changes due to repetitive fMRI scans. Another limitation of this study is that the examiners were unmasked, which may be a source of bias. In addition, although our subjects were college students, future experiments should use a stronger accommodative target to measure NPC and PFV at near. The vision therapy that has been studied within the randomized clinical trial of CITT includes accommodative training, which this study did not include. Eye movement recordings should also be recorded simultaneously with fMRI, which was not incorporated due to the cost of an fMRI compatible eye movement monitor.

CONCLUSIONS

This pilot investigation study is an important first step in understanding how the vision therapy protocol described within this research evoked clinical and functional cortical changes in the four

CI subjects studied. NPC, RPC, PFV at near, and near dissociated phoria improved. The average peak velocity from 2 and 4° convergence step stimuli increased. By using a prediction vs. random fMRI experimental protocol, increases in the spatial extent and the average correlation within an ROI were observed in the frontal lobe region (containing FEF, SEF, and DLPFC), the parietal area, the cerebellum, and the brain stem. Several clinical parameters were positively correlated with the changes in cortical activity. Causality cannot be addressed within this study because of the limited number of subjects and the type of analyses conducted. Future studies should include larger populations and analyses such as Granger causality as correlation analysis is not appropriate to investigate causal relationships. Our data also showed that convergent peak velocities to symmetrical 4° step stimuli were significantly slower in CI subjects compared with controls but divergent movements to symmetrical 4° step stimuli were not significantly different. These results add evidence that convergence and divergence are different systems.

Future Direction

Future research should include a detailed analysis dissecting the vergence eye movements throughout vision therapy. We speculate that the increased peak velocity observed through vision therapy may be from an increase in the preprogrammed transient component described by the Dual Model Theory.⁷² Vergence has been described using the Dual Mode Theory to control two components: a transient preprogrammed element that facilitates the movement's speed corresponding to the burst cells recorded from the midbrain and a feedback controlled element that enables the system to be very accurate corresponding to the burst tonic cells also recorded from the midbrain.⁷² Our laboratory and others have shown that the peak velocity of vergence can be increased or decreased using step-ramp,⁷³ double step,⁷⁴ and large step³² stimuli during an adaptation experiment in controls with normal binocular vision. Our group has also shown that slow ramp stimuli influence the feedback portion of the vergence movement.⁷⁵ Future research should be conducted to investigate the underlying neural control of the system to attain a better understanding of the neural control components that are changing during vision therapy. The rate and type of vision therapy may affect the transient and sustained component differently. For example, CITT has shown that rate of improvement is more rapid for NPC and PFV at near compared with symptoms in children undergoing treatment for CI.⁷⁶

Furthermore, future studies should include controls with normal binocular vision through vision therapy and incorporate a placebo therapy for controls and patients with CI. When a placebo therapy is studied, we can determine if the fMRI changes are due to adaptation from vision therapy or a motor learning effect from multiple scans. Future research directions should also include more subjects and control interventions to determine if the results reported here continue in a larger population. Subjects' symptoms should be quantified with the validated CISS at the time of testing.^{27–29}

Phoria adaptation has been shown to be decreased in CI subjects compared with controls,⁷⁷ and it is improved after vision therapy.⁵² Hence, quantifying eye movement with fMRI during a phoria adaptation experiment could yield insight into what cortical

changes are correlated to the improved ability to perform phoria adaptation.

A detailed investigation could also be performed to understand mechanisms initially used by a subject to compensate for CI. For example, the subject may use saccades to increase vergence peak velocity and/or suppression. It is also unknown if these compensation mechanisms potentially change during therapy and if the adaptation is maintained long-term.

ACKNOWLEDGMENTS

We thank John L. Semmlow for comments on the initial manuscript and Diana Ludlam for the design of the home training protocol.

This research was supported in part by NSF CAREER BES-044713 (to TLA), NIH 5R01NS049176 (to BBB), and NIH 5R01NS055808 and 5K02NS047099-6 (to AMB). The contents of this article were developed under a grant from the Department of Education, NIDRR Grant H133P090009 (to NC) but do not necessarily represent policy of the Department of Education.

None of the authors within this manuscript have commercial associations with the research that could result in a conflict of interest.

Received March 29, 2010; accepted August 24, 2010.

REFERENCES

1. Rouse MW, Hyman L, Hussein M, Solan H. Frequency of convergence insufficiency in optometry clinic settings. Convergence Insufficiency and Reading Study (CIRS) Group. *Optom Vis Sci* 1998;75:88–96.
2. Scheiman M, Gallaway M, Coulter R, Reinstein F, Ciner E, Herzberg C, Parisi M. Prevalence of vision and ocular disease conditions in a clinical pediatric population. *J Am Optom Assoc* 1996;67:193–202.
3. Rouse MW, Borsting E, Hyman L, Hussein M, Cotter SA, Flynn M, Scheiman M, Gallaway M, De Land PN. Frequency of convergence insufficiency among fifth and sixth graders. The Convergence Insufficiency and Reading Study (CIRS) group. *Optom Vis Sci* 1999;76:643–9.
4. Hokoda SC. General binocular dysfunctions in an urban optometry clinic. *J Am Optom Assoc* 1985;56:560–2.
5. Porcar E, Martinez-Palomera A. Prevalence of general binocular dysfunctions in a population of university students. *Optom Vis Sci* 1997;74:111–3.
6. Goodrich GL, Kirby J, Cockerham G, Ingalla SP, Lew HL. Visual function in patients of a polytrauma rehabilitation center: a descriptive study. *J Rehabil Res Dev* 2007;44:929–36.
7. Brahm KD, Wilgenburg HM, Kirby J, Ingalla S, Chang CY, Goodrich GL. Visual impairment and dysfunction in combat-injured servicemembers with traumatic brain injury. *Optom Vis Sci* 2009;86:817–25.
8. Stelmack JA, Frith T, Van Koeveing D, Rinne S, Stelmack TR. Visual function in patients followed at a Veterans Affairs polytrauma network site: an electronic medical record review. *Optometry* 2009;80:419–24.
9. Ciuffreda KJ, Kapoor N, Rutner D, Suchoff IB, Han ME, Craig S. Occurrence of oculomotor dysfunctions in acquired brain injury: a retrospective analysis. *Optometry* 2007;78:155–61.
10. Cohen M, Groswasser Z, Barchadski R, Appel A. Convergence insufficiency in brain-injured patients. *Brain Inj* 1989;3:187–91.
11. Suchoff IB, Kapoor N, Waxman R, Ference W. The occurrence of ocular and visual dysfunctions in an acquired brain-injured patient sample. *J Am Optom Assoc* 1999;70:301–8.
12. Scheiman M, Rouse M, Kulp MT, Cotter S, Hertle R, Mitchell GL. Treatment of convergence insufficiency in childhood: a current perspective. *Optom Vis Sci* 2009;86:420–8.

13. Convergence Insufficiency Treatment Trial (CITT) Study Group. The Convergence Insufficiency Treatment Trial: design, methods, and baseline data. *Ophthalmic Epidemiol* 2008;15:24–36.
14. Pickwell LD, Hampshire R. The significance of inadequate convergence. *Ophthalmic Physiol Opt* 1981;1:13–8.
15. Daum KM. Convergence insufficiency. *Am J Optom Physiol Opt* 1984;61:16–22.
16. Grisham JD. Visual therapy results for convergence insufficiency: a literature review. *Am J Optom Physiol Opt* 1988;65:448–54.
17. Rouse M, Borsting E, Mitchell GL, Kulp MT, Scheiman M, Amster D, Coulter R, Fecho G, Gallaway M. Academic behaviors in children with convergence insufficiency with and without parent-reported ADHD. *Optom Vis Sci* 2009;86:1169–77.
18. Birnbaum MH, Soden R, Cohen AH. Efficacy of vision therapy for convergence insufficiency in an adult male population. *J Am Optom Assoc* 1999;70:225–32.
19. Scheiman M, Cotter S, Rouse M, Mitchell GL, Kulp M, Cooper J, Borsting E. Randomised clinical trial of the effectiveness of base-in prism reading glasses versus placebo reading glasses for symptomatic convergence insufficiency in children. *Br J Ophthalmol* 2005;89:1318–23.
20. Scheiman M, Mitchell GL, Cotter S, Kulp MT, Cooper J, Rouse M, Borsting E, London R, Wensveen J. A randomized clinical trial of vision therapy/orthoptics versus pencil pushups for the treatment of convergence insufficiency in young adults. *Optom Vis Sci* 2005;82:583–95.
21. Scheiman M, Mitchell GL, Cotter S, Cooper J, Kulp M, Rouse M, Borsting E, London R, Wensveen J. A randomized clinical trial of treatments for convergence insufficiency in children. *Arch Ophthalmol* 2005;123:14–24.
22. Randomized clinical trial of treatments for symptomatic convergence insufficiency in children. *Arch Ophthalmol* 2008;126:1336–49.
23. Yuan W, Semmlow JL. The influence of repetitive eye movements on vergence performance. *Vision Res* 2000;40:3089–98.
24. Ciuffreda KJ, Rutner D, Kapoor N, Suchoff IB, Craig S, Han ME. Vision therapy for oculomotor dysfunctions in acquired brain injury: a retrospective analysis. *Optometry* 2008;79:18–22.
25. Previc FH. Functional specialization in the lower and upper visual fields in humans: its ecological origins and neurophysiological implications. *Behav Brain Sci* 1990;13:519–75.
26. Weiss PH, Marshall JC, Wunderlich G, Tellmann L, Halligan PW, Freund HJ, Zilles K, Fink GR. Neural consequences of acting in near versus far space: a physiological basis for clinical dissociations. *Brain* 2000;123(Pt 12):2531–41.
27. Rouse MW, Borsting EJ, Mitchell GL, Scheiman M, Cotter SA, Cooper J, Kulp MT, London R, Wensveen J. Validity and reliability of the revised Convergence Insufficiency Symptom Survey in adults. *Ophthalmic Physiol Opt* 2004;24:384–90.
28. Rouse M, Borsting E, Mitchell GL, Cotter SA, Kulp M, Scheiman M, Barnhardt C, Bade A, Yamada T. Validity of the Convergence Insufficiency Symptom Survey: a confirmatory study. *Optom Vis Sci* 2009;86:357–63.
29. Borsting EJ, Rouse MW, Mitchell GL, Scheiman M, Cotter SA, Cooper J, Kulp MT, London R. Validity and reliability of the revised Convergence Insufficiency Symptom Survey in children aged 9 to 18 years. *Optom Vis Sci* 2003;80:832–8.
30. Horng JL, Semmlow JL, Hung GK, Ciuffreda KJ. Initial component control in disparity vergence: a model-based study. *IEEE Trans Biomed Eng* 1998;45(2):249–57.
31. Bahill AT, Kallman JS, Lieberman JE. Frequency limitations of the two-point central difference differentiation algorithm. *Biol Cybern* 1982;45:1–4.
32. Alvarez TL, Bhavsar M, Semmlow JL, Bergen MT, Pedrono C. Short-term predictive changes in the dynamics of disparity vergence eye movements. *J Vis* 2005;5:640–9.
33. Alvarez TL, Semmlow JL, Yuan W, Munoz P. Comparison of disparity vergence system responses to predictable and unpredictable stimulations. *Curr Psychol Cogn* 2002;21:243–61.
34. Cox RW. AFNI: software for analysis and visualization of functional magnetic resonance neuroimages. *Comput Biomed Res* 1996;29:162–73.
35. D'Esposito M, Zarahn E, Aguirre GK, Rypma B. The effect of normal aging on the coupling of neural activity to the bold hemodynamic response. *Neuroimage* 1999;10:6–14.
36. Oakes TR, Johnstone T, Ores Walsh KS, Greischar LL, Alexander AL, Fox AS, Davidson RJ. Comparison of fMRI motion correction software tools. *Neuroimage* 2005;28:529–43.
37. Logothetis NK, Wandell BA. Interpreting the BOLD signal. *Annu Rev Physiol* 2004;66:735–69.
38. Attwell D, Iadecola C. The neural basis of functional brain imaging signals. *Trends Neurosci* 2002;25:621–5.
39. Calhoun VD, Kiehl KA, Pearlson GD. Modulation of temporally coherent brain networks estimated using ICA at rest and during cognitive tasks. *Hum Brain Mapp* 2008;29:828–38.
40. Gavrilescu M, Stuart GW, Rossell S, Henshall K, McKay C, Sergejew AA, Copolov D, Egan GF. Functional connectivity estimation in fMRI data: influence of preprocessing and time course selection. *Hum Brain Mapp* 2008;29:1040–52.
41. Berns GS, Song AW, Mao H. Continuous functional magnetic resonance imaging reveals dynamic nonlinearities of “dose-response” curves for finger opposition. *J Neurosci* 1999;19:RC17.
42. Beckmann CF, Smith SM. Probabilistic independent component analysis for functional magnetic resonance imaging. *IEEE Trans Med Imaging* 2004;23:137–52.
43. Talairach J, Tournoux P. *Co-Planar Stereotaxic Atlas of the Human Brain: 3-Dimensional Proportional System: An Approach to Cerebral Imaging*. New York, NY: Thieme Medical Publishers; 1988.
44. Ward BD. Simultaneous Inference for FMRI Data. 2000. Available at: <http://afni.nimh.nih.gov/afni/download/afni/releases/latest>. Accessed September 24, 2010.
45. Lewis JW, Brefczynski JA, Phinney RE, Janik JJ, DeYoe EA. Distinct cortical pathways for processing tool versus animal sounds. *J Neurosci* 2005;25:5148–58.
46. Schmid A, Rees G, Frith C, Barnes G. An fMRI study of anticipation and learning of smooth pursuit eye movements in humans. *Neuroreport* 2001;12:1409–14.
47. Binder JR, Liebenthal E, Possing ET, Medler DA, Ward BD. Neural correlates of sensory and decision processes in auditory object identification. *Nat Neurosci* 2004;7:295–301.
48. Kennedy DN, Lange N, Makris N, Bates J, Meyer J, Caviness VS Jr. Gyri of the human neocortex: an MRI-based analysis of volume and variance. *Cereb Cortex* 1998;8:372–84.
49. Griffin JR. *Binocular Anomalies Procedures For Vision Therapy*, 2nd ed. Chicago, IL: Professional Press; 1988.
50. CITT Study Group. Long-term effectiveness of treatments for symptomatic convergence insufficiency in children. *Optom Vis Sci* 2009;86:1096–103.
51. Sloan JA, Cella D, Hays RD. Clinical significance of patient-reported questionnaire data: another step toward consensus. *J Clin Epidemiol* 2005;58:1217–9.
52. Brautaset RL, Jennings AJ. Effects of orthoptic treatment on the CA/C and AC/A ratios in convergence insufficiency. *Invest Ophthalmol Vis Sci* 2006;47:2876–80.
53. Cohen AH, Soden R. Effectiveness of visual therapy for convergence insufficiencies for an adult population. *J Am Optom Assoc* 1984;55:491–4.

54. Milder DG, Reinecke RD. Phoria adaptation to prisms. A cerebellar-dependent response. *Arch Neurol* 1983;40:339–42.
55. Nitta T, Akao T, Kurkin S, Fukushima K. Involvement of the cerebellar dorsal vermis in vergence eye movements in monkeys. *Cereb Cortex* 2008;18:1042–57.
56. Morley JW, Judge SJ, Lindsey JW. Role of monkey midbrain near-response neurons in phoria adaptation. *J Neurophysiol* 1992;67:1475–92.
57. Kim EH, Granger-Donetti B, Vicci VR, Alvarez TL. The relationship between phoria and the ratio of convergence peak velocity to divergence peak velocity. *Invest Ophthalmol Vis Sci* 2010;51:4017–27.
58. Han SJ, Guo Y, Granger-Donetti B, Vicci VR, Alvarez TL. Quantification of heterophoria and phoria adaptation using an automated objective system compared to clinical methods. *Ophthalmic Physiol Opt* 2010;30:95–107.
59. Chen YF, Lee YY, Chen T, Semmlow JL, Alvarez TL. Behaviors, models, and clinical applications of vergence eye movements. *J Med Biol Engin* 2010;30:1–15.
60. Lee YY, Granger-Donetti B, Chang C, Alvarez TL. Sustained convergence induced changes in phoria and divergence dynamics. *Vision Res* 2009;49:2960–72.
61. van Leeuwen AF, Westen MJ, van der Steen J, de Faber JT, Collewyn H. Gaze-shift dynamics in subjects with and without symptoms of convergence insufficiency: influence of monocular preference and the effect of training. *Vision Res* 1999;39:3095–107.
62. Ungerleider LG, Mishkin M. Two cortical visual systems. In: Ingle DJ, Goodale MA, Mansfield RJW, eds. *Analysis of Visual Behavior*. Cambridge, United Kingdom: MIT Press; 1982:549–86.
63. Takagi M, Tamargo R, Zee DS. Effects of lesions of the cerebellar oculomotor vermis on eye movements in primate: binocular control. *Prog Brain Res* 2003;142:19–33.
64. Sander T, Sprenger A, Neumann G, Machner B, Gottschalk S, Rambold H, Helmchen C. Vergence deficits in patients with cerebellar lesions. *Brain* 2009;132:103–15.
65. Gamlin PD, Yoon K. An area for vergence eye movement in primate frontal cortex. *Nature* 2000;407:1003–7.
66. Alvarez TL, Alkan Y, Suril G, Ward BD, Biswal BB. Functional anatomy of predictive vergence and saccadic eye movements in humans: a functional MRI investigation. *Vision Res* 2010;50:2163–75.
67. Mays LE. Neural control of vergence eye movements: convergence and divergence neurons in midbrain. *J Neurophysiol* 1984;51:1091–108.
68. Patel SS, Jiang BC, White JM, Ogmen H. Nonlinear alteration of transient vergence dynamics after sustained convergence. *Optom Vis Sci* 1999;76:656–63.
69. Lee YY, Chen T, Alvarez TL. Quantitative assessment of divergence eye movements. *J Vis* 2008;8:5.1–13.
70. Alvarez TL, Semmlow JL, Pedrono C. Dynamic assessment of disparity vergence ramps. *Comput Biol Med* 2007;37:903–9.
71. Teitelbaum B, Pang Y, Krall J. Effectiveness of base in prism for presbyopes with convergence insufficiency. *Optom Vis Sci* 2009;86:153–6.
72. Hung GK, Semmlow JL, Ciuffreda KJ. A dual-mode dynamic model of the vergence eye movement system. *IEEE Trans Biomed Eng* 1986;33:1021–8.
73. Yuan W, Semmlow JL, Alvarez TL, Munoz P. Dynamics of the disparity vergence step response: a model-based analysis. *IEEE Trans Biomed Eng* 1999;46:1191–8.
74. Takagi M, Oyamada H, Abe H, Zee DS, Hasebe H, Miki A, Usui T, Hasegawa S, Bando T. Adaptive changes in dynamic properties of human disparity-induced vergence. *Invest Ophthalmol Vis Sci* 2001;42:1479–86.
75. Alvarez TL, Semmlow JL, Yuan W, Munoz P. Dynamic details of disparity convergence eye movements. *Ann Biomed Eng* 1999;27:380–90.
76. Scheiman M, Kulp MT, Cotter S, Mitchell GL, Gallaway M, Boas M, Coulter R, Hopkins K, Tamkins S. Vision therapy/orthoptics for symptomatic convergence insufficiency in children: treatment kinetics. *Optom Vis Sci* 2010;87:593–603.
77. Brautaset RL, Jennings JA. Horizontal and vertical prism adaptation are different mechanisms. *Ophthalmic Physiol Opt* 2005;25:215–8.

Tara L. Alvarez, PhD

*Department of Biomedical Engineering
New Jersey Institute of Technology, University Heights
Newark, New Jersey 07102
e-mail: tara.l.alvarez@njit.edu*

Bharat B. Biswal, PhD

*Department of Radiology
UMDNJ - New Jersey Medical School, University Heights
Newark, New Jersey 07103
e-mail: bbiswal@gmail.com*